ELSEVIER

Chemical Engineering Journal 135 (2008) 168–173

Chemical Engineering Journal

www.elsevier.com/locate/cej

Review

Syntheses of ZnO and ZnO-coated TiO_2 nanoparticles in various alcohol solutions at multibubble sonoluminescence (MBSL) condition

Ki-Taek Byun [a], Kook Won Seo [b], Il-Wun Shim [b], Ho-Young Kwak [a,*]

[a] *Department of Mechanical Engineering, Chung-Ang University, Seoul 156-756, Republic of Korea*
[b] *Department of Chemistry, Chung-Ang University, Seoul 156-756, Republic of Korea*

Received 12 February 2007; received in revised form 21 March 2007; accepted 28 March 2007

Abstract

Syntheses of zinc oxide (ZnO) and ZnO-coated titanium dioxide nanoparticles under ultrasonic field at the multibubble sonoluminescence (MBSL) condition were tried in various alcohol solutions. The MBSL condition facilitates the supercritical state of liquid layer where high-energy chemical reaction in the layer around the bubble is possible. At the optimal MBSL condition in alcohol solutions containing zinc acetate dihydrate of 2.75 wt%, sodium hydroxide of 1 wt% and TiO_2 of 1 wt%, ZnO nanoparticles having the average diameter of 7 nm were synthesized first and subsequently ZnO-coated TiO_2 nanoparticles were synthesized within 10 min. The prepared particles of ZnO and ZnO-coated TiO_2 were examined by XRD, UV–vis spectrophotometer and HR-TEM.

Keywords: ZnO nanoparticles; ZnO-coated TiO_2 nanoparticles; Multibubble sonoluminescence (MBSL); Supercritical state

1. Introduction

Zinc oxide (ZnO) powder which has been used as primary reinforcing filler for elastomers was produced by gas phase synthesis in flame [1]. Last 10 years or so, however, various preparation methods of ZnO nanoparticles [2–6] and their size dependent electronic [7] and optical [8] properties have been studied extensively for specific applications such as catalysts, photovoltaic and electroluminescent devices and functional devices (sensor, varistor, etc.). However, a precise control of homogeneity, particle size and shape of ZnO by sophisticated manufacturing process is needed for the specific applications.

Various methods such as microemulsion-mediated process [2], laser evaporation and subsequent condensation [3], a modified sol–gel procedure with metal alkoxides [5], flow spray pyrolysis (FSP) [6], reversed-micelles (RM) method [4] and precipitation from zinc acetate in various alcohol solutions [9] were tried to synthesize specialty ZnO nanoparticles. In general, the physical and chemical properties of the ZnO nanoparticles are different depending on the manufacturing method. For example, gas phase synthesis in flame is suitable for the relatively higher crystallinity of the particles, while a wet process such as precipitation of zinc salt and post calcinations provides larger specific surface area [5]. On the other hand, the ZnO powder from FSP of zinc salt aqueous solution has comparable BET equivalent particle diameter but has higher crystallinity than the ones from the wet process of sol–gel procedure [5]. Such experimental result indicates that the ZnO powder from FSP has combined characteristics of the powder prepared from gas phase synthesis and the wet procedure.

Previously, amorphous iron [10], palladium [11] nanoparticles and metal alloys [12] have been prepared by ultrasonic irradiation of solutions containing volatile transition metal carbonyls. Also, pure Fe_3O_4 nanoparticles were synthesized by simple sonication of iron(II) acetate in water [13]. However, more homogeneous metal oxide nanoparticles were found to be synthesized within 10 min at the multibubble sonoluminescence (MBSL) condition. On the other hand, it took more than 10 h to obtain the same amount of product by simple ultrasonic irradiation. Furthermore, various core/shell type nanocrystals turned out to be synthesized only at this condition [14].

In this study, ZnO and ZnO-coated TiO_2 nanoparticles were synthesized by the ultrasonic irradiation of zinc salt solution with NaOH at the multibubble sonoluminescence condition in various alcohol solutions. The intense local heating in the liquid adjacent to the bubble wall at the collapse point is expected to provide

* Corresponding author. Tel.: +82 2 820 5278; fax: +82 2 826 7464.
E-mail address: kwakhy@cau.ac.kr (H.-Y. Kwak).

1385-8947/$ – see front matter © 2007 Elsevier B.V. All rights reserved.
doi:10.1016/j.cej.2007.03.085

similar reaction condition which could be obtained from the FSP of zinc salt solution. The estimated temperature and pressure in the liquid layer are about 1000 °C and 500 bar [15], respectively, which make high-energy chemical reaction possible to produce novel materials with unusual properties [16–18]. Especially, the MBSL condition facilitates the supercritical state of liquid layer where the acceleration of any chemical reactions is possible [19]. In fact, the XRD pattern for the ZnO particles synthesized at the MBSL condition is quite similar to that of the ZnO particles by FSP. Also, the size and size distribution depending on the solvent were investigated in this study.

2. Experimental

2.1. Synthesis

The solvents used are ethanol (C_2H_5OH, 99.5%, Aldrich), 1-propanol ($CH_3CH_2CH_2OH$, 99.7%, Aldrich), 1-butanol ($CH_3(CH_2)_3OH$, 99.8%, Aldrich), 1-pentanol ($CH_3(CH_2)_4OH$, 99%, Aldrich) and 1-hexanol ($CH_3(CH_2)_5OH$, 98%, Aldrich) and were used as received.

Zinc oxide (ZnO) powder was synthesized by ultrasonic radiation at the MBSL condition. An experimental apparatus for the MBSL consists of a cylindrical quartz cell into which a 5 mm diameter titanium horn (Misonix XL2020, USA) is inserted, as shown in Fig. 1. The system operates at 20 kHz and power input of 200 W. The solution in the test cell was kept at constant pressure with argon atmosphere. Continuous circulation of water to the bath in which the cell is immersed keeps the temperature of the solution inside the cell around 25 °C. The MBSL condition can be found by trial and error at a proper ultrasound intensity, liquid temperature and distance between the horn tip and the bottom of the cell.

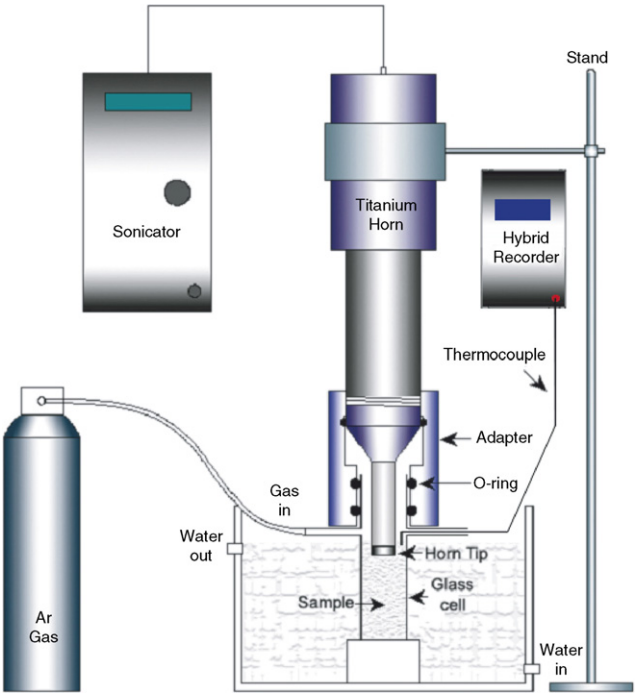

Fig. 1. Experimental set-up for MBSL experiment.

A solution was made by the addition of 4 mmol sodium hydroxide (NaOH, 99.99%, Aldrich) to 2 mM zinc acetate dihydrate ($Zn(CH_3CO_2)_2{\cdot}2H_2O$, 99.999%, Aldrich) solution in the experimental cell. The solution was sonicated at the MBSL condition for about 5 min to obtain zinc oxide powder. In all cases the products were collected by centrifugation (Hanil, HM-150IV, Korea) and washed with deionized water and dried in oven for 10 h.

For the coating of ZnO onto TiO_2 nanoparticles, 2 mmol zinc acetate dehydrate, 4 mmol sodium hydroxide and 2 mmol TiO_2 (Degussa, P-25, average size of 21 nm in diameter) in distilled water (13 ml) were sonicated at the aforementioned MBSL condition. After 20 min later, the resulting powder was prepared. These resulting particles were washed by DI-water in order and dried in oven for 12 h.

2.2. Physical characterization

Zinc oxide powder samples were characterized by X-ray diffractometer (Scintag XDS-2000, $\lambda = 1.5418$ Å, USA) and infrared spectroscopy (Nicolet Model Impact 400D, KBr pellets, 4 cm^{-1} resolution). The morphology of the product was determined by high precision transmission electron microscopy (JEOL, JFM-3000F, Japan). Prepared zinc oxide powder in various alcohol solution at the MBSL condition was monitored by UV–vis spectroscopy (Hitachi, U-3300), obtaining the absorption spectra for ZnO colloids in methanol. Measurement of photoluminescence generated by using a laser at 365 nm was also performed.

3. Results and discussion

Fig. 2 shows the XRD patterns of ZnO nanoparticles synthesized from zinc acetate dehydrate ($Zn(CH_3CO_2)_2{\cdot}2H_2O$, 99.999%, Aldrich) in various alcohol solutions with sodium

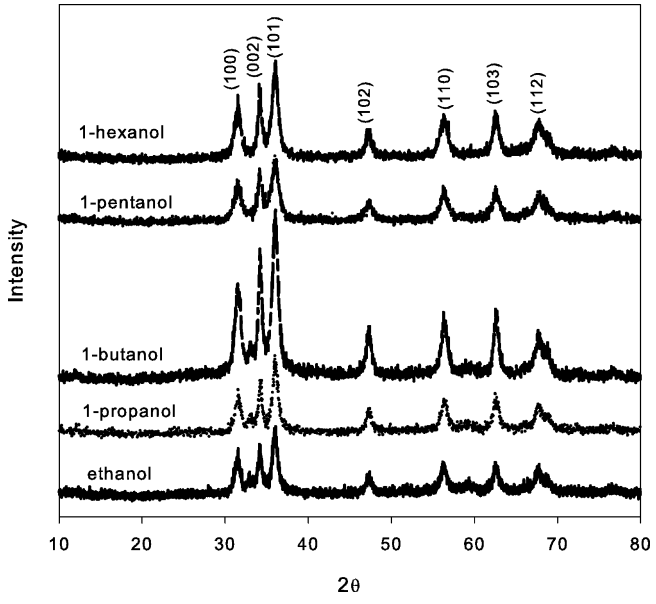

Fig. 2. XRD pattern for ZnO powder prepared in various alcohol solutions with NaOH at the MBSL condition.

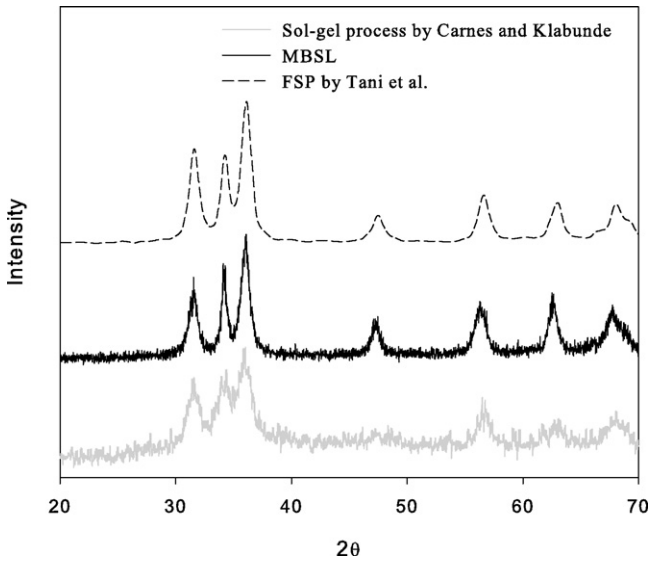

Fig. 3. XRD patterns for ZnO powder prepared by various processes: (a) sol–gel process after heat treating at 600 °C (—), (b) sonochemistry at the MBSL condition (—) and FSP (– – –).

hydroxide (NaOH, 99.99%, Aldrich) at the MBSL condition. In all these cases, the positions of all characteristic peaks occur at $2\theta = 31.5, 34.3, 36.1, 47.3, 56.0, 62.7$ and 67.6° corresponding to (1 0 0), (0 0 2), (1 0 1), (1 0 2), (1 1 0), (1 0 3) and (1 1 2) planes. The XRD patterns of all powders indicate hexagonal zincite (JCPDS #36-1451), which has also slight peaks of $2\theta = 66.2$ and 69.0° around $2\theta = 67.6^\circ$, as shown in Fig. 2. However, the relative intensity at $2\theta = 34.3^\circ$ is greater than that at $2\theta = 31.47^\circ$, which is the only difference from the XRD pattern for the commercial ZnO particles [5]. Rather, the XRD pattern is similar to the one for the ZnO powder produced by a modified sol–gel process and subsequent heat treatment at about 700 °C [5] as shown in Fig. 3. For comparison, the XRD patterns for the ZnO particles obtained from the sol–gel process after heat treatment at 600 °C [5] and FSP [6] along with our results in 1-hexanol solution are given in Fig. 3. Our XRD pattern is also very similar to the one by FSP where the maximum flame temperature is estimated to be about 2200–2600 K [20].

There was no great solvent effect in synthesizing the ZnO powder. The mean crystallite size diameter (D) of the ZnO particles was estimated by the following Scherrer's formula [21]

$$D = \frac{0.9\lambda}{B\cos\theta_B} \tag{1}$$

where λ is the X-ray wavelength, B the full-width at half maximum and θ_B represents the diffraction angle at a certain crystal plane. The estimated diameters of ZnO particles prepared in various alcohol solutions using Eq. (1) with the (1 0 0) peak are shown in Table 1. The average diameter of 7.1 nm obtained in this study is close to the value obtained by spray pyrolysis using a filter expansion aerosol generator [22], however, the diameter is about half of the one by FSP [6] or by the microemulsion-mediated process [2]. Slight decrease in the particle size can be seen when the ZnO particle is prepared in the longer chain length alcohol solution.

Table 1
Calculated diameter of ZnO particle prepared in various alcohol solutions using Scherrer's formula at the diffraction angle $\theta_B = 15.735^\circ$ and using Brus equation with the wavelength at the inflection point

Solvent	B (rad)	Calculated diameter (nm)	
		Scherrer's formula	Brus equation
Ethanol	0.018	8.18	8.24
1-Propanol	0.020	7.38	7.82
1-Butanol	0.022	6.61	6.77
1-Pentanol	0.023	6.41	6.37
1-Hexanol	0.021	7.03	7.54

Fig. 4 shows absorption spectra obtained from the colloid of ZnO nanoparticles prepared in various alcohol solutions. The colloids were made by mixing 0.1 g of prepared ZnO powder with 10 ml methanol. All the absorbance spectra exhibit a well-defined exciton peak around 352–357 nm, showing that the average particle size is in the quantum regime. The average particle size in a colloid may be obtained from the wavelength at the inflection point after the exciton peak [23] which provides the band gap of the particle, $E_g = hc/\lambda$. Since the band gap of the particle E_g can be estimated by the following effective mass model [24], one can calculate the average particle size of the colloid

$$E_g = E_g^{bulk} + \frac{h^2}{8r^2 m_0}\left(\frac{1}{m_e^*} + \frac{1}{m_h^*}\right) - \frac{1.8e^2}{4\pi\varepsilon\varepsilon_0 r} - \frac{0.124 m_0 e^4}{\hbar^2(4\pi\varepsilon_0)^2\varepsilon^2} \times \left[\left(\frac{1}{m_e^*} + \frac{1}{m_h^*}\right)\right]^{-1} \tag{2}$$

where E_g^{bulk} is the bulk band gap (eV), $\hbar$ the Planck's constant, r the particle radius, m_e is the electron effective mass, m_h the hole effective mass, m_0 the free electron mass, e the charge on the electron, ε the relative permittivity and ε_0 is the permittivity of free space. With $m_e = 0.26$, $m_h = 0.59$, $\varepsilon = 8.5$ and $E_g^{bulk} = 3.2$ eV and with the wavelength at the inflection point,

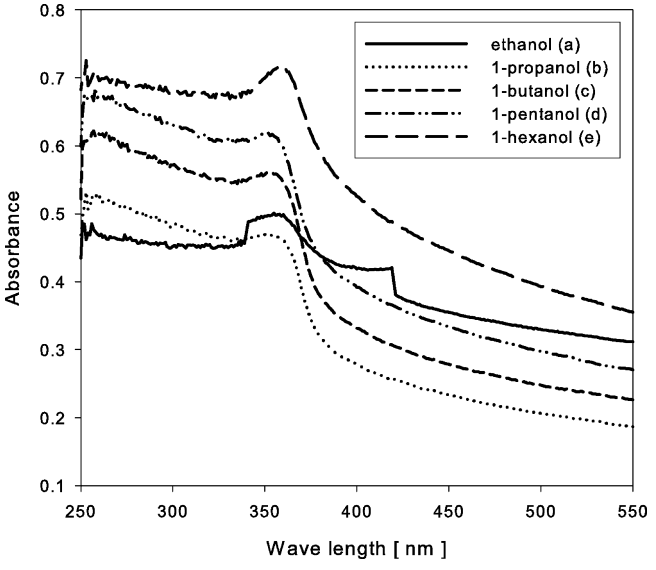

Fig. 4. UV–vis spectroscopy from the ZnO colloids in methanol solution.

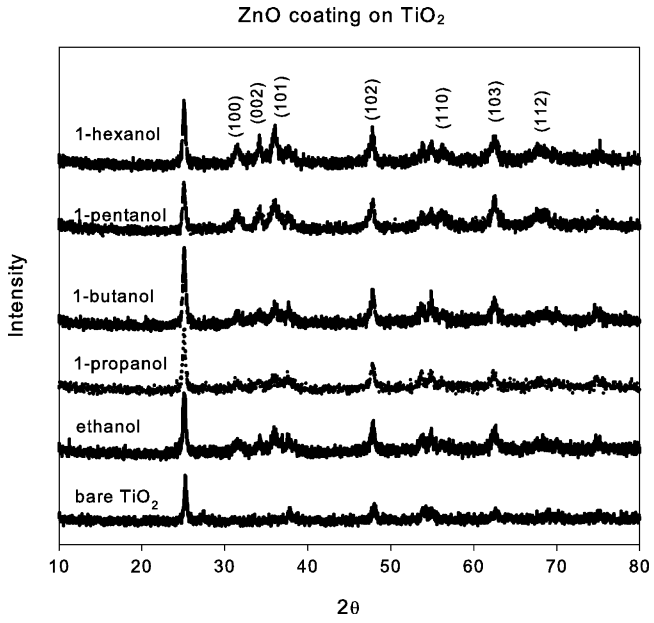

Fig. 5. XRD pattern for ZnO-coated TiO_2 nanoparticles prepared in various alcohol solutions.

the average particle diameter estimated by Eq. (2) is about 7.2 nm in diameter. As can be seen in Table 1, the diameters of ZnO particles obtained from the Brus equation are in good agreement with the value obtained from the XRD data.

Fig. 5 shows the XRD pattern of the ZnO-coated TiO_2 nanoparticles prepared in various alcohol solutions at the MBSL condition. Similar intense peaks for ZnO as shown in Fig. 2 appear with less intensity, which indicates that the particles are nano-sized and the ZnO is thinly coated on TiO_2. Typical peaks for TiO_2 at $2\theta = 24.93, 48.53^\circ$ are also shown in Fig. 5.

Fig. 6a shows a transmission electron microscope image of ZnO particles prepared in 1-butanol solution. From the lattice fringe, one can find that the particle shape is spherical and the diameter of the particle is about 6.3 nm which is close to the particle diameter of 7.1 nm estimated by the Scherrer's formula, as shown in Table 1. Fig. 6b and c shows a transmission electron microscope image of ZnO-coated TiO_2 nanoparticles. The average size of the bare TiO_2 nanoparticles was about 21 nm and those of ZnO-coated TiO_2 nanoparticles were found to be about 30 nm range.

Fig. 7 shows the room temperature photoluminescence (PL) spectrum of the ZnO powder synthesized in various solutions at the MBSL condition. The PL spectrum is very broad, with a

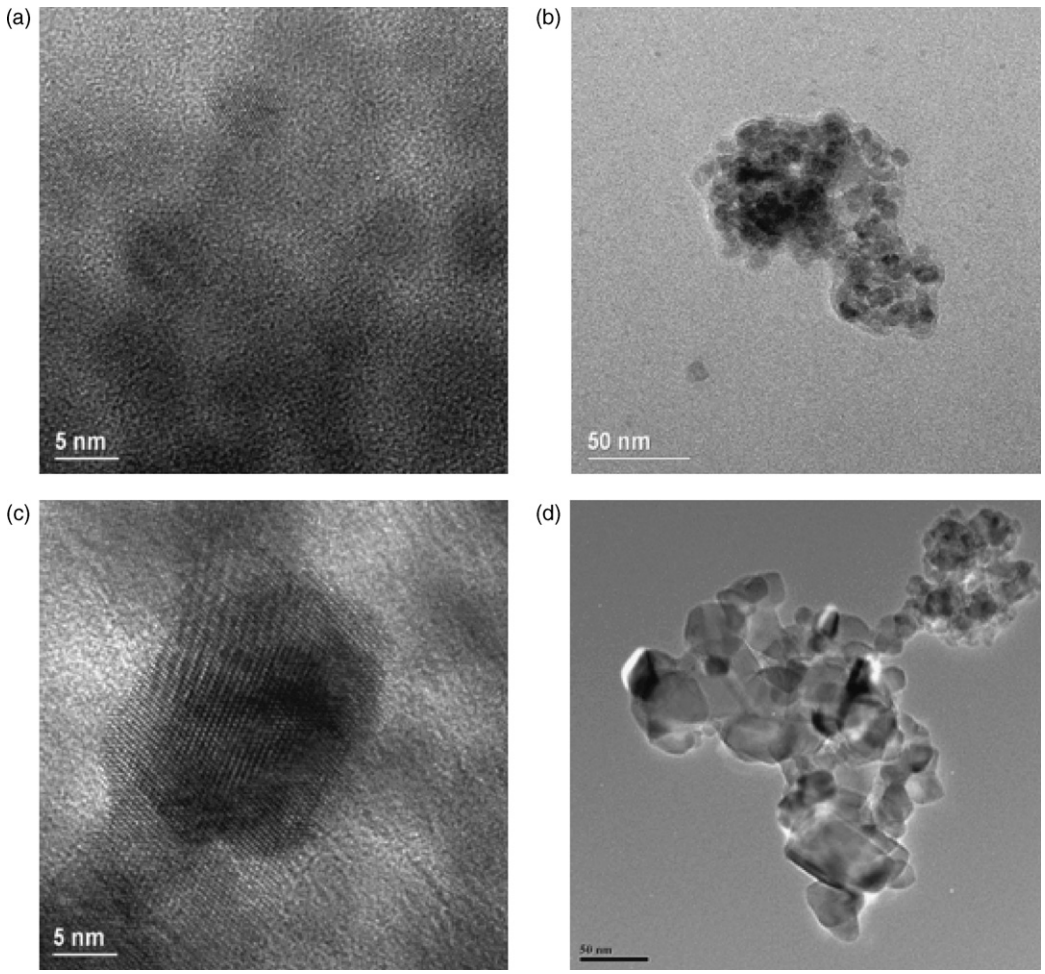

Fig. 6. TEM images of: (a) ZnO particles, (b and c) HR-TEM image of ZnO-coated TiO_2 particles prepared in 1-butanol solution and (d) HR-TEM image of bare TiO_2 particles.

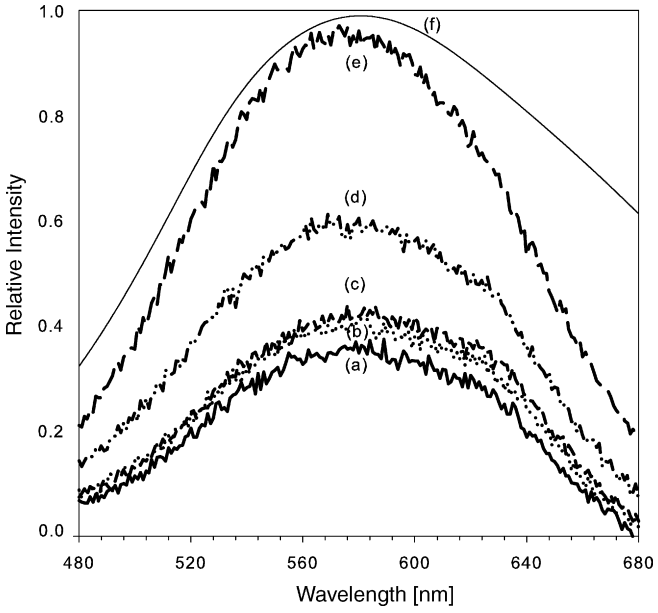

Fig. 7. Photoluminescence spectra from ZnO prepared in various alcohol solutions: (a) ethanol, (b) 1-propanol, (c) 1-butanol, (d) 1-pentanol and (e) 1-hexanol at the MBSL condition and from an aged ZnO prepared by sol–gel process (f).

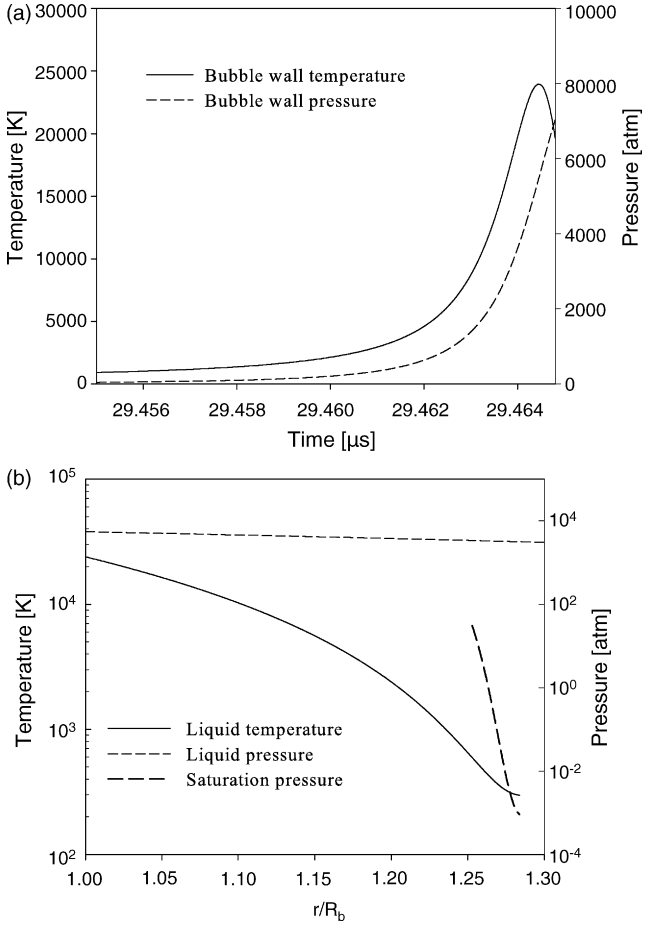

Fig. 8. (a) Time-dependent bubble wall temperature and pressure around the collapse point. (b) Calculated temperature and pressure distribution in the liquid layer adjacent to the bubble wall for the argon bubble with equilibrium radius of 10 μm driven at 1.3 atm and at 20 kHz.

maximum centered at 580 nm, which is slightly higher than that of the aged sample prepared by the sol–gel process [25]. The red shifted emission band peak from 500 nm for a fresh powder to 560 nm after aging is due to the increase in the cluster sizes from 3.5 to 5.5 nm in diameter during aging process. It is reasonable to obtain PL spectrum with a maximum at 580 nm from the ZnO powder having size of 7 nm in diameter.

Fig. 8a shows the time-dependent temperature and pressure at the bubble wall around the collapse point and Fig. 8b shows spatial temperature and pressure distributions in the liquid layer adjacent to the bubble wall at the collapse point for and argon bubble with an equilibrium radius of 10 μm driven at the ultrasound amplitude of 1.3 atm and frequency of 20 kHz. As can be seen from Fig. 8b, the pressure value at the point where the temperature is 610 K, the critical temperature of 1-hexanol is much greater than the critical pressure of 1-hexanol, 33.8 atm, so that the supercritical state of 1-hexanol is developed above $T = 610$ K. Below 610 K, the pressure values are always greater than the saturation pressure corresponding to the temperature so that no evaporation takes place in the liquid layer. The estimated duration of supercritical state of 1-hexanol from Fig. 8a is about 2 ns. Rapid syntheses of ZnO in various solutions at the MBSL condition might be due to the existence of transient supercritical state near the collapse point at the MBSL condition. In fact, much higher reaction rate of the hydrolysis of *p*-nitrophenyl acetate by several orders of magnitude in the presence of ultrasound was considered to be attributed to the existence of transient supercritical state of water during the bubble collapse [26].

4. Conclusion

Wurtzite phase ZnO nanoparticles of about 7 nm in particle diameter were synthesized sonochemically at the multibubble sonoluminescence condition in various alcohol solutions. Compared with the other preparation methods, the sonochemical method at MBSL condition produces ZnO nanoparticle with the smallest and the most homogeneous in primary particle diameter. The synthesized ZnO nanoparticles may be used for varistor and photovoltaic devices and ZnO-coated TiO_2 nanoparticles may be used for a material to reduce the recombination loss in dye solar cell unit.

Acknowledgments

This work has been supported by a grant from Electric Power Research Institute (EPRI) in USA, under contract EP-P19394/C9578, and by the Seoul R&BD program (2006).

References

[1] S.V. Teague, O.G. Raabe, Generation of fume aerosols of zinc oxide, Am. Ind. Hyg. Assoc. J. 41 (1980) 680–683.
[2] S. Hingorani, V. Pillai, P. Kumar, M.S. Multani, D.O. Shah, Microemulsion mediated synthesis of zinc-oxide nanoparticles for varistor studies, Mater. Res. Bull. 28 (1993) 1303–1310.
[3] M.S. El-Shall, D. Graiver, U. Pernisz, M.I. Baraton, Synthesis and characterization of nanoscale zinc oxide particles: I. Laser vaporization/condensation technique, Nanostruct. Mater. 6 (1995) 297–300.

[4] D. Kaneko, H. Shouji, T. Kawai, K. Kon-No, Synthesis of ZnO particles by ammonia-catalyzed hydrolysis of zinc dibutoxide in nonionic reversed micelles, Langmuir 16 (2000) 4086–4089.
[5] C.L. Carnes, K.J. Klabunde, Synthesis, isolation, and chemical reactivity studies of nanocrystalline zinc oxide, Langmuir 16 (2000) 3764–3772.
[6] T. Tani, L. Mädler, S.E. Pratsinis, Homogeneous ZnO nanoparticles by flame spray pyrolysis, J. Nanopart. Res. 4 (2002) 337–343.
[7] M.F. Iskandar, K. Okuyama, F.G. Shi, Stable photoluminescence of zinc oxide quantum dots in silica nanoparticles matrix repaired by the combined sol–gel and spray drying method, J. Appl. Phys. 89 (2001) 6431–6434.
[8] M. Abdullah, S. Shibamoto, K. Okuyama, Synthesis of ZnO/SiO_2 nanocomposites emitting specific luminescence colors, Opt. Mater. 26 (2004) 95–100.
[9] Z. Hu, G. Oskam, P.C. Searson, Influence of solvent on the growth of ZnO nanoparticles, J. Colloid Interface Sci. 263 (2003) 454–460.
[10] K.S. Suslick, S. Choe, A.A. Cichowlas, M.W. Grinstaff, Sonochemical synthesis of amorphous iron, Nature 353 (1991) 414–416.
[11] N.A. Das, H. Cohen, A. Gedanken, In situ preparation of amorphous carbon-activated palladium nanoparticles, J. Phys. Chem. B 101 (1997) 6834–6838.
[12] K.S. Suslick, T. Hyeon, M. Fang, A.A. Cichowlas, Sonochemical synthesis of nanostructured catalysts, Mater. Sci. Eng. A 204 (1995) 186–192.
[13] R. Vijayakumar, Yu. Koltypin, I. Felner, A. Gedanken, Sonochemical synthesis and characterization of pure nanometer-sized Fe_3O_4 particles, Mater. Sci. Eng. A 186 (2000) 101–105.
[14] S.S. Lee, K.W. Seo, S.H. Yoon, I. Shim, K. Byun, H. Kwak, CdS coating on TiO_2 nanoparticles under multibubble sonoluminescence condition, Bull. Korean Chem. Soc. 26 (2005) 1579–1581.
[15] H. Kwak, H. Yang, An aspect of sonoluminescence from hydrodynamic theory, J. Phys. Soc. Jpn. 64 (1995) 1980–1992.
[16] K.S. Suslick, M.M. Fang, T. Hyeon, M.M. Mdleleni, Sonochemistry and Sonoluminescence, Kluwer Academic Publishers, Netherlands, 1999, pp. 291–320.
[17] F. Grieser, Encyclopedia of Surface and Colloid Science, Marcel Dekker, New York, 2002, pp. 4760–4774.
[18] S.S. Manoharan, M.L. Rao, Encyclopedia of Nanoscience and Nanotechnology, vol. 10, American Scientific Publishers, California, 2004, pp. 67–82.
[19] I. Hua, R.H. Höchemer, M.R. Hoffmann, Sonolytic hydrolysis of *p*-nitrophenyl acetate: the role of supercritical water, J. Phys. Chem. 99 (1995) 2335–2342.
[20] L. Mädler, H.K. Kammler, R. Muller, S.E. Pratsinis, Controlled synthesis of nanostructured particles by flame spray pyrolysis, J. Aerosol. Sci. 33 (2002) 369–389.
[21] H.P. Klug, L.E. Alexander, X-ray Diffraction Procedures, John Wiley and Sons, New York, 1974.
[22] Y.C. Kang, S.B. Park, Effect of preparation conditions on the formation of primary ZnO particles in filter expansion aerosol generator, J. Mater. Sci. Lett. 16 (1997) 131–133.
[23] N.S. Pesika, K.J. Stebe, P.C. Searson, Determination of the particle size distribution of quantum nanocrystals from absorbance spectra, Adv. Mater. 15 (2003) 1289–1291.
[24] L. Brus, Electronic wave functions in semiconductor clusters: experiment and theory, J. Phys. Chem. 90 (1986) 2555–2560.
[25] L. Spanhel, M.A. Anderson, Semiconductor clusters in the sol–gel process: quantized aggregation, gelation, and crystal growth in concentrated zinc oxide colloids, J. Am. Chem. Soc. 113 (1991) 2826–2833.
[26] H. Hung, M.R. Hoffmann, Kinetics and mechanism of the sonolytic degradation of chlorinated hydrocarbons: frequency effects, J. Phys. Chem. A 103 (1999) 2734–2739.